Energy & Buildings 208 (2020) 109660

Contents lists available at ScienceDirect

Energy & Buildings

journal homepage: www.elsevier.com/locate/enbuild

Analyses of different operation modes of pumping and recharging well using an indoor sandbox test

Wei Song[a,*], Long Ni[b,*], Yang Yao[b]

[a] School of Civil and Engineering, North China University of Technology, Beijing 100144, PR China
[b] School of Architecture, Harbin Institute of Technology, Harbin 150090, PR China

ARTICLE INFO

Article history:
Received 13 June 2019
Revised 16 November 2019
Accepted 1 December 2019
Available online 1 December 2019

Keywords:
Groundwater
Heat pump system
Pumping and recharging well
Experimental sandbox
Aquifer
Continuous operation

ABSTRACT

A pumping and recharging well (PRW) system is an important single well groundwater heat pump system that is being used increasingly in practical projects such as in renewable energy utilization systems. In this study, we investigated four different PRW operation modes based on the heating and cooling periods in Shenyang, Beijing, and Shanghai using the physical simulation experimental sandbox of a single well groundwater heat pump that can accurately reflect actual physical phenomena. In the experiment, the duration of the operating conditions is distributed according to heating, air conditioning, and recovery seasons. The experiments were conducted under four conditions: continuous heating (CH), continuous cooling (CC), first summer then winter (SW), and first winter then summer (WS). In the heating/cooling load-dominant areas, the results show that an aquifer cannot be restored to its original state during the natural recovery period. In the CH/CC conditions, the cumulative heat absorption and rejection in six cycles decreases by 23.0% and 6.0%, respectively. The results also show that the PRW is more sensitive in the heating mode and heat absorption is more difficult than heat rejection. In the CH condition, the effect of the initial disturbance on the aquifer is more evident. The reduction in the cumulative heat in the second operating cycle is 57.1% of the total reduction in the six cycles. Thus, it is necessary to continue recharging the aquifer over time based on the building load to ensure long-term reliable operation of the system. In the heating/cooling load-dominant districts, the use of the SW operation mode can improve system stability. The results of the study offer valuable practical reference for implementing PRWs and can be applied to aquifer energy storage.

1. Introduction

Ground source heat pump (GSHP) systems are being increasingly applied in practical projects as renewable energy utilization systems. Groundwater heat pump systems are ideal solutions for heating and cooling buildings because of their advantages. When groundwater is used as the primary energy source in combination with a heat pump, the groundwater is pumped from a pumping area, heated/cooled in the heat exchanger of the heat pump, and then injected into an irrigation area. The single well groundwater heat pump (SWGWHP) is a new type of groundwater heat pump, which has become increasingly popular because of its economic advantages. In general, SWGWHPs comprise a standing column well (SCW), pumping and recharging wells (PRWs), and a forced external circulation SCW (FECSCW) [1].

Previous studies on SWGWHP focused on formulating a heat transfer model, heat transfer characteristics simulation, economic evaluation, and so on. In recent years, experimental studies and mathematical modeling have been carried out on a single well geothermal heating system to predict its performance; the results show that the average extracted thermal output is 448.49 kW and 413.63 kW in the first and tenth heating cycles, respectively [2]. Lee compared and analyzed experimental data of different types of rocks, borehole depths, injection heat values, and effective thermal conductivity in a standing column well and found that groundwater flow clearly affects thermal conductivity [3]. Through experimental and numerical analysis, it was reported that the thermal conductivity of SCW improved by approximately 165.4% and 186.8% at a bleeding rate of 10% and a maximum bleeding rate of 30%, respectively [4]. A 3D unsteady-state multi-scale model considering fluid flow and heat transfer processes of a single well system was developed. The results of this model indicate that a longer interval could effectively eliminate the early breakthrough of circulating fluid [5].

* Corresponding authors.
E-mail addresses: stillwater2013@163.com (W. Song), nilonggn@163.com (L. Ni).

https://doi.org/10.1016/j.enbuild.2019.109660
0378-7788/

According to previous research on thermal features of the three types of thermal wells, PRWs have obvious advantages because a middle partition area exists in a PRW such that backwater is completely injected into an aquifer, whereas thermal transfixion occurs rarely [6]. In view of the increasing complexity of operational performance, the current related research on GSHP focused on system characteristics and energy consumption. However, the gradual shift to system operation analysis has motivated researchers in the field of heat pumps to increasingly focus on the problems of different operation modes for both short- and long-term operations.

Mohammad [7] investigated different operation modes and used finite element numerical simulation to evaluate the performance of a ground thermal storage system with various types of soils and pump operations. Zvonimir [8] developed a mathematical model of a liquid-to-water heat pump system to analyze the performance of domestic hot water production and found that the use of a liquid–vapor heat exchanger is beneficial because it leads to high coefficients of performance. Kang [9] configured a complementary combined cooling, heating, and power-organic Rankine cycle system with a GSHP based on thermal and electricity demands to analyze the operational cost and system efficiency. Zhang [10] introduced a new multi-period model considering three geographical locations with different heating and cooling demands to improve the cost effectiveness and thermodynamic efficiency of heat pump systems.

A review of heat pumps in European district heating reveals several types of heat pump connections and operations, such as heat pumps with a single heat source, with thermal energy storage, and with multistage operation [11]. A three-dimensional finite element model of a helical coil ground heat exchanger (GHE) was developed to analyze a single GHE and multiple GHEs. The intermittent short-time operating mode improved the GHE performance [12]. The operating characteristics of an air source and a solar energy multi-functional heat pump system under various working modes were analyzed to provide a reference for further operation optimization [13]. The performance of a multi-heat pump was measured and analyzed in four operation modes by adjusting the control parameters [14]. The thermal performance of three types of vertical GHEs with two operation modes was investigated, and it was found that their heat exchange rates had different characteristics [15].

Researchers have investigated the long-term performance of solar-assisted ground-coupled heat pump (SAGCHP) systems, particularly in cold winter areas. Dai [16] conducted an experimental study on the influence of operation modes on the heating performance of an SAGCHP system. Stojanovic [17] presented the two-year performance of an SAGCHP system for heating under Nordic climatic conditions and an optimized control and operation strategy. Francesco [18,19] developed a new control strategy for an SAGCHP system to analyze the energy consumption of solar collectors and GHEs. Moreover, the study focused on different control strategies for a solar-assisted GSHP (SAGSHP) system for cold climates and a dynamic simulation approach was applied using TRNSYS. The continuous operation of an SAGCHP system was simulated for 20 years under the meteorological conditions in Beijing using TRNSYS. The simulation results showed that the long-term yearly average space heating efficiency increased by 26.3% compared with that of a conventional GSHP system [20]. In another study, four different types of heat pump systems were analyzed using a mathematical model in a 30-year operating period considering variations in the building loads, ambient air temperature, soil temperature, and coefficient of performance (COP) of the GCHP [21].

Long-term operation of GSHP system has been extensively investigated. Hassam [22] proposed three configurations of various community-sized solar heating systems and showed that an average renewable energy fraction of 53–81% could be achieved. To predict the long-term performance of GHEs, Babak [23] formulated a new one-dimensional analytical expression for the heat transfer rate using the g-function method, which was validated using experimental data. An integrated predictive model was developed to assess the long-term performance of GSHP systems. The model completely considered dynamic heat loads, the energy consumption by accessories, and the three-dimensional dynamic heat transfer process in GHEs [24]. Choi [25] assessed the effect of the long-term operation of GSHP systems for 10 years of operation and found that the surface boundary condition plays an important role in long-term simulation. The thermal performance of two office buildings was investigated through long-term computer simulation, and it was found that reducing the heat imbalance on the ground side is a key factor that limits the effect of thermal drift [26]. A long-term dynamic coupling model was developed to determine the effect of GSHP systems on variations in the soil temperature. It was shown that the soil temperature would increase by 2.56–3.00 °C after 15 years, and the inlet water temperature in summer would be 36 °C after nine years [27]. A novel model was developed to calculate the soil temperature distribution and COP of GSHPs, including the seasonal balance between heat absorption and heat rejection in 10 years [28]. A three-dimensional dynamic simulation experiment platform was used to evaluate the performance of GCHP under Harbin, Shenyang, and Beijing thermal load, and to analyze the annual COP of the system under Beijing thermal load in the 10th year [29]. A real retrofit project with 16 borehole heat exchangers was implemented using steady-state thermal response step testing to analyze long-term GCHP efficiency, and the borehole temperature and COP variations for 30 years were simulated [30].

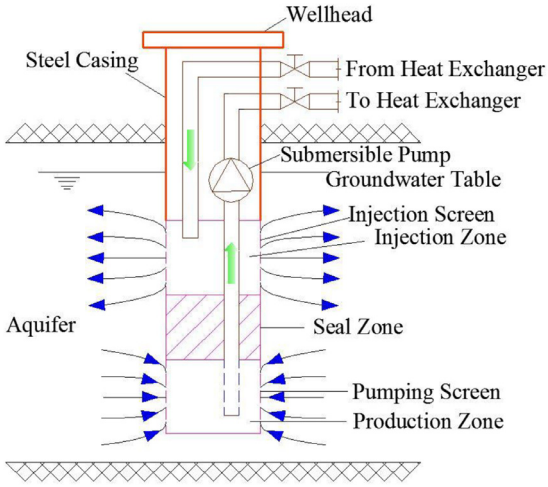

Fig. 1. Schematic of a pumping and recharging well (PRW).

Long-term performance prediction is important because the efficiency of a GHE decreases based on the lifetime of the system. A series of simulations was performed to evaluate the long-term sustainability and efficiency of FECSCWs, and the winter–summer and winter modes were analyzed for 30 years [31]. To evaluate the thermal performance, a mathematical model was established to analyze the groundwater seepage of a single-well circulation system, and it was found that the long-term development of the outlet temperature fluctuates annually [32]. For few laboratory experiments, this study is the first to investigate the long-term operation of PRW under different operating conditions, which used a PRW (Fig. 1) as the research object in three cities, namely Shenyang, Beijing, and Shanghai, representing severe cold, cold, and hot summer/cold winter regions, respectively. The PRW was experimentally investigated in four operation modes: continuous heating (CH),

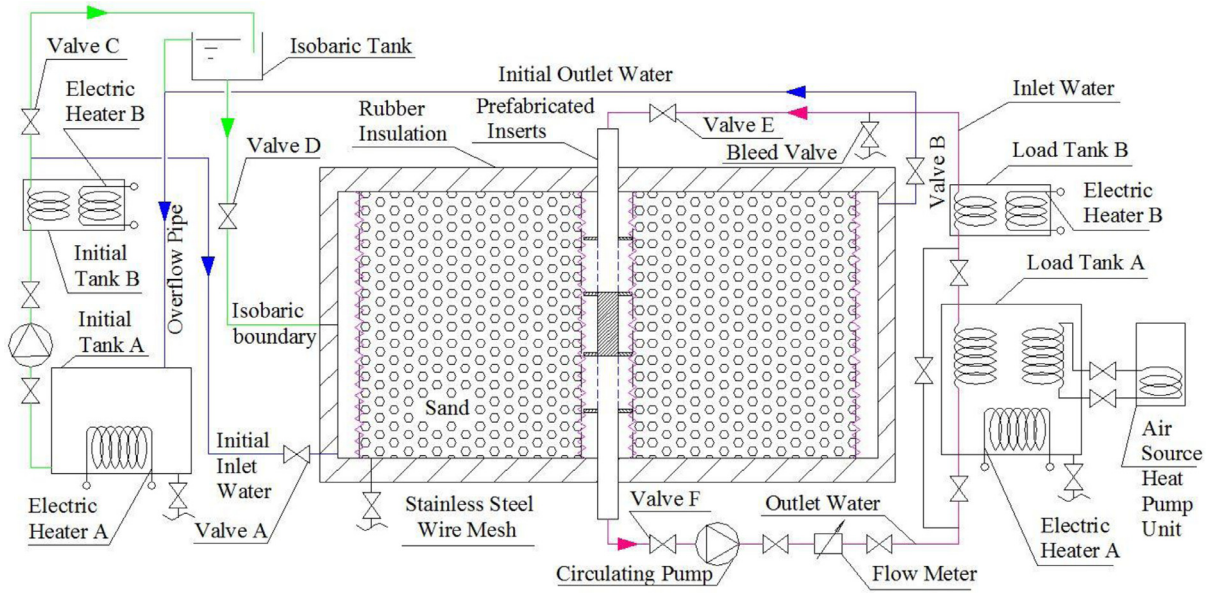

Fig. 2. Test system diagram.

Table 1
Details of the experimental system.

Contents	Units	Values
Sand tank	m	1.5 × 1.5 × 1[a]
Initial tank A	m	0.7 × 0.7 × 0.7[a]
Load tank A	m	1 × 1 × 1[a]
Isobaric tank	m	0.4 × 0.4 × 0.8[a]
Electric heater A	kW	1
Electric heater B	kW	0.5
Air source heat pump unit	kW	2.5
Circulating pump	kW	0.28
Diameter of well	mm	73
Diameter of inserts	mm	22
Diameter of sand	mm	1–2
Diameter of gravel	mm	2–4
Length of well	m	0.92
Length of inserts	m	1.5

a Length × Width × Height.

continuous cooling (CC), first summer then winter (SW), and first winter then summer (WS).

2. Experimental setup

2.1. Experiment description

The experimental system was designed as presented in Fig. 2 and Table 1 to study the heat transfer performance and variation in the temperature of the PRW during the process of pumping water from the bottom of the well to the top. The experimental system consists of a sand tank with confined water to approximate an aquifer, two load tanks to simulate the building load, two initial tanks to control the initial aquifer temperature, an isobaric tank to maintain the water level and the pressure of water in the sand tank, and an air source heat pump unit to cool water in the load tank. Other details of the experimental system are presented in Table 1. The pumping and injection screens are each 150 mm in length, whereas the distance between the pumping and injection screens is 300 mm, as shown in Fig. 3.

In the sand tank experiment, groundwater was pumped out from the bottom of the simulated well using a circulating pump. Then, a heat exchange process occurs between the groundwater

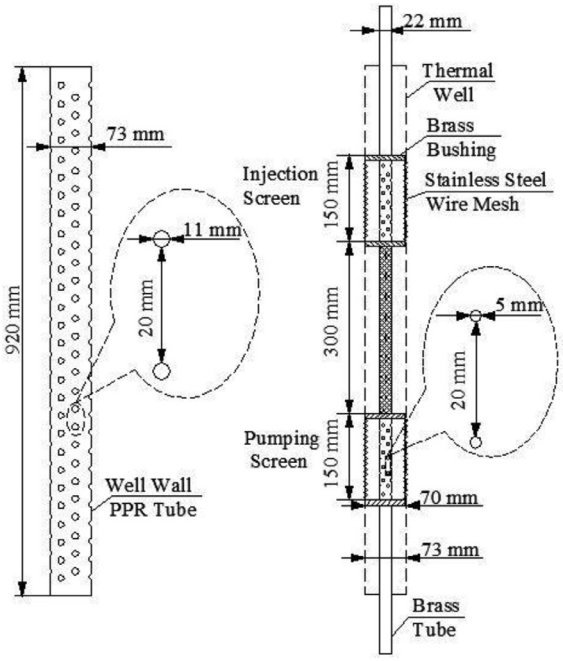

Fig. 3. Structure of the thermal well and prefabricated insert.

and the cold/hot water in load tanks A and B to simulate the building load. To determine the characteristics of the PRW, 32 copper–constantan thermocouples (T-type) and 20 pressure points (capillary) located at different positions in the system were used to measure the distributions of the temperature and pressure. There are 24 thermocouples in the sand tank; thus, the distribution of the inner temperature can be easily observed. In addition, a turbine flow meter was installed at the outlet water pipe to measure the water flow rate. The above-mentioned measurement processes were monitored and controlled using a data acquisition system (National Instruments), which includes NI PXIe-1073, NI PXI-6224, and NI PXIe-4353.

It is difficult to simulate the geological conditions of different regions by replacing the aquifer in the sandbox owing to the limitations of the experimental conditions. Therefore, the conditions

were simulated using the same sand to analyze their effects on the characteristics of the PRW under different modes of operation. The durations of different operating conditions for the same operation mode were selected based on the durations of the heating, air conditioning, and recovery periods in Shenyang, Beijing, and Shanghai [33]. The influence of climatic conditions on the aquifer temperature, which is closely related to the initial aquifer temperature, was neglected; however, for a given building load, variation in the aquifer temperature is weakly correlated with its initial temperature. Thus, the initial aquifer temperature remains constant during the experiment. The building load of this bench is significantly different from that of actual GSHP systems.

In practice, the capacity of the thermal source well should meet the requirement of the building load, which is related to architectural functions, climatic and geological conditions, and so forth; however, it is unrelated to the initial aquifer temperature and non-repeatable. In this experiment, the building load was generated by the groundwater extracted from the load water tank, which exchanges heat with the cold/hot water in the load water tank. Thus, the building load is strongly related to the initial aquifer temperature. When the cold/hot water temperature in the load water tank remains essentially constant, the building load does not significantly change if the initial aquifer temperature is constant. Therefore, the building load is approximately constant, and it is easy to highlight the effect of the operation mode. For the ease of expression, the name of Shenyang, Beijing, and Shanghai were used to indicate the experimental conditions of different running times. In addition, to evaluate the influence of different operation modes on the system, the proportion of time scales was appropriately expanded under the experimental conditions, and we ensured that the boundary conditions of the bench were not affected.

2.2. Test procedure

(1) First, the pre-well to be tested was installed in a flask, and water required by the aquifer was produced at the initial geothermal temperature using the original and fine-tuning water tanks (initial tanks A and B).
(2) When the initial water temperature in the original water tank was achieved, the flask was filled with water by opening valves A and B by displacing air bubbles from the bottom and slowly filling the tank with water. The internal temperature of the flask was adjusted to the initial temperature to achieve the desired experimental conditions, and a uniform distribution was maintained. The procedure lasted approximately 24 h.
(3) When the aquifer temperature meets the test conditions, valves A and B were closed, whereas valves C and D were opened. Overflow was achieved using the high water tank to supply water. The control head should be kept constant to maintain a stable sand box pressure.
(4) The experiment was initiated by maintaining a constant pressure in the isobaric tank, opening valves E and F of the inlet and outlet of the thermal source well, and turning the circulating pump, as shown in Fig. 2.

2.3. Experimental conditions

To simulate the annual conditions of a PRW under eight conditions, the temperatures of the load tank were set as 4 °C and 30 °C for heat removal/exothermic conditions, the initial aquifer temperature was set as 20 °C, the flow rate of the circulating water pump was set as 0.54 m^3/h, and the pressure of the flask filled with water was 17.4 kPa. In the experiment, the durations of heating and air conditioning were allocated for Shenyang, Beijing, and Shanghai, as listed in Table 2.

Table 2
Heating and air conditioning seasons of the simulation region.

		Beijing	Shenyang	Shanghai
Heating season	Date (M-D)	11-08–03-02	10-29–03-22	12-08–02-15
	Days (d)	115	145	70
Air conditioning season	Date (M-D)	06-11–09-08	07-01–09-08	05-22–10-18
	Days (d)	90	70	150

As stated earlier, the experiment was conducted in four operation modes: CH, CC, SW, and WS. Each mode was divided into six cycles of 120 min. The start and stop times of each mode were based on the duration of heating, air conditioning, and the recovery periods in the three areas. The durations for each condition are listed in Table 3.

The experimental duration for simulating 8760 h within an entire year is only 53 min as the geometric ratio of the sandbox bench is 1:100. Moreover, the duration of each operating condition is less than 15 min because of the winter heating period, the summer air conditioning period, and two convalescent periods. To evaluate the influence of different operation modes on the PRW, the cumulative heat extraction and release quantities must be moderately increased based on the experiment expanded time. In addition, the distal boundaries of the sandbox bench should not be affected. Hence, the duration of one experiment was doubled to approximately 120 min. Consequently, the time ratio of each condition increased to 1:4320, with 120 min simulating one year of actual operation.

2.4. Uncertainty analysis

Uncertainties in any experiment can arise because of instrument selection, instrument condition, instrument calibration, environmental conditions, etc. Thus, uncertainty analysis is required to verify the accuracy of the experiments [34]. The uncertainty analysis in these experiments includes the error estimations for both measured and calculated parameters. The measured parameters include the temperature, flow rate, and time, and their errors are the measurement errors.

The uncertainties δx_i and relative uncertainties δRx_i of the measured parameters can be obtained from the following equations:

$$\delta x_i = A \cdot \gamma_i \tag{1}$$

$$\delta Rx_i = \frac{\delta x_i}{x_i} \tag{2}$$

where A is the upper limit of the measuring range, and γ_i is the accuracy grade, as provided by the manufacturer.

The calculated parameters include cumulative heat absorption and cumulative heat rejection, and these can be calculated using Eq. (3). Here, Q is the heat absorption/rejection quantity of the thermal well in kJ, C_w is the volumetric heat capacity of water in kJ/(m^3 °C), V_w is the flow rate of outlet water in m^3/s, T_o is the outlet water temperature in °C, T_i is the inlet water temperature in °C, and t is the duration of the entire experiment in minutes.

The basic root-sum-square (RRS) method introduced by Moffat [35] is used to evaluate the relative uncertainty of the calculated parameters. The RRS method is described as follows:

If a parameter F is a function of a series of measured independent variables x_i, the relative uncertainty δRF for F can be obtained from Eq. (4). The relative uncertainties with regard to the typical values of the main parameters are listed in Table 4.

$$Q = C_w V_w (T_o - T_i) t \tag{3}$$

Table 3
Time distribution of each operating condition.

Simulation location	Operation Mode	Winter (min)	Recovery (min)	Summer (min)	Recovery (min)
Shenyang	CH	48.3	71.7	–	–
Shanghai	CC	–	–	50	70
Beijing	SW WS	38.3	31.7	30	20
Shenyang	SW WS	48.3	31.4	23.3	17
Shanghai	SW WS	23.3	30	50	16.7

Table 4
Total uncertainty of the measured parameters and experimental results.

Parameters	Type of data	Unit	CH Condition		CC Condition	
			Typical value	Relative uncertainty	Typical value	Relative uncertainty
Inlet water temperature to PRW, T_i	Measured	°C	11.73	1.20%	28.58	1.20%
Outlet water temperature to PRW, T_o	Measured	°C	16.68	1.00%	23.55	1.00%
Flow rate of outlet water, V_w	Measured	m^3/h	0.54	0.60%	0.54	0.60%
Test time, t	Measured	min	48.3	0.035%	50.0	0.033%
Heat absorption quantity, Q	Calculated	kJ	8890.02	6.70%	–	–
Heat rejection quantity, Q	Calculated	kJ	–	–	9636.37	5.655%

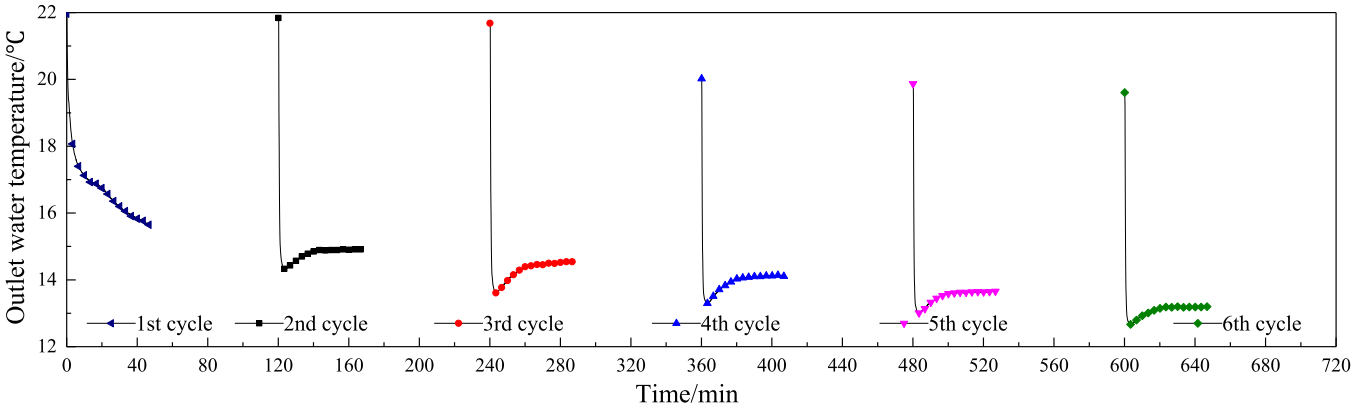

Fig. 4. Temperature of the outlet water under the continuous heating (CH) condition.

$$\delta RF = \frac{\sqrt{\sum_{i=1}^{n}\left(\frac{\partial F_i}{\partial x_i}\delta x_i\right)^2}}{F} \quad (4)$$

3. Results and discussion

3.1. Experimental features of continuous heating

Fig. 4 shows variations in the water temperature in the six cycles under the CH condition. The working conditions were applied in the experiment based on the heating and air conditioning periods in Shenyang. Each cycle of the heating period in winter was 48.3 min, and the recovery time was 71.7 min. As shown in Fig. 4, the pumping temperature in the six cycles has a downward trend. This indicates that during the simulation of six years with PRW, the extraction temperature of the PRW decreases yearly owing to lack of supplementary heat in the underground aquifer for natural restoration. Although the temperature of each cycle decreases every year, in each cycle, the temperature first decreases and then slightly increases, except for the first cycle in which the temperature only decreases. It is considered that in the first period of the experiment, the thermal source well bears a larger load, causing its pumping temperature to gradually decrease. However, in the second to the sixth operating cycles, its temperature remains almost constant after the system becomes stable. In addition, in these cycles, the heat provided by the underground aquifer is the same as the simulated building load; this does not lead to a decrease in the pumping temperature. Thus, it can be inferred that if the experiment is continued under the same conditions and no additional heat is introduced to supplement the aquifer, the outlet water temperature of the PRW will continue to decline.

Fig. 5 shows variations in the average temperature of the outlet and inlet water of the PRW in the six cycles under continuous heat removal conditions. The average temperature of the PRW decreases every year in the six cycles. In the six-year simulated system operation, the average temperature of the thermal source well gradually decreases from 16.7 °C in the first cycle to 13.1 °C in the sixth cycle (a reduction of 21.6%), and the average inlet water temperature gradually decreases from 11.7 °C in the first cycle to 9.3 °C in the sixth cycle (a reduction of 20.5%). This shows that the PRW simulates the operation of heating load-dominant regions. Underground aquifers cannot be restored to their original state in the natural recovery period. A decrease in the average outlet water temperature will affect the efficiency of heat pump systems. Therefore, it is necessary to examine the decrease in this temperature in that type of district every year, and appropriate measures must be implemented to supplement heat for the underground aquifers in a timely manner to prevent abnormal operation of the heat pump system.

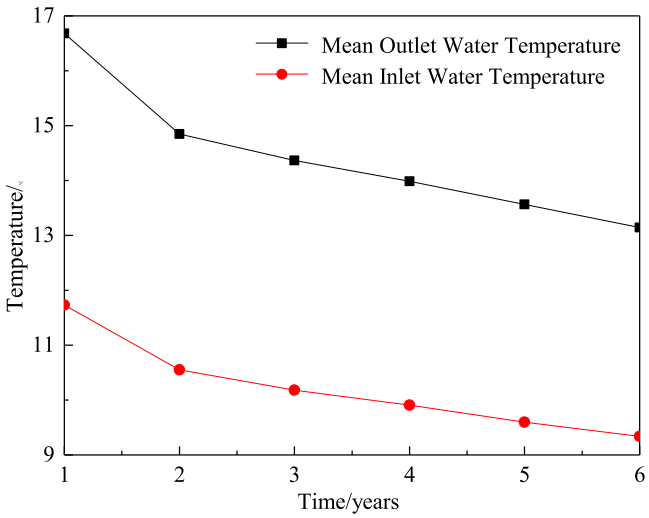

Fig. 5. Mean temperatures of the outlet and inlet water under the CH condition.

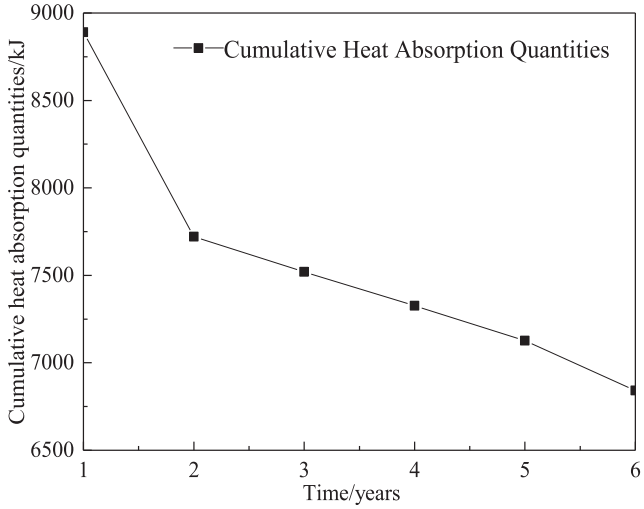

Fig. 6. Cumulative heat absorption quantities under the CH condition.

The changes in the cumulative heat quantities in the six cycles under the CH condition are shown in Fig. 6. The cumulative heat extraction and the average outlet water temperature of the PRW show a decreasing trend in the six cycles. In the six-year simulated system operation, the cumulative heat of the thermal source well gradually decreases from 8890.0 kJ in the first cycle to 6841.1 kJ in the sixth cycle (a reduction of 23.0%). The cumulative heat extracted in the second running cycle is 7720.6 kJ, and the cumulative heat extracted in the first running cycle decreased by 1169.4 kJ (a reduction of 57.1%). This is the reason for the continuous decrease in the pumping temperature in the first running cycle.

3.2. Experimental features of continuous cooling

Fig. 7 shows variations in the outlet water temperatures in the six cycles under the CC condition. The conditions were set based on the durations of the heating and air conditioning periods in Shanghai. The heat release time in summer is 50 min, and the recovery period is 70 min. As shown in Fig. 7, the outlet water temperatures in the six cycles gradually rise. It can be observed that during the simulation of the PRW for six years, the outlet water temperature of the PRW rises every year owing to the insufficient cooling capacity provided by natural recovery in the underground aquifer. Fig. 7 also shows that the outlet water temperature of the thermal source well increases in each cycle. The cooling capacity provided by the underground aquifer does not meet the simulated building load, leading to a sharp rise in the pumping temperature. In other words, the pumping temperature of the system will continue to increase if the experimental conditions remain the same as there is no other cooling capacity to supplement the aquifer.

Fig. 8 shows variations in the average outlet and inlet water temperatures in the six cycles under continuous heat emission conditions. The average outlet and inlet water temperatures of the PRW increase every year in the six cycles. In the six-year simulated system operation, the average pumping temperature of the thermal source well gradually increases from 21.1 °C in the first cycle to 25.6 °C in the sixth cycle (an increase of 21.3%), and the average backflow water temperature of the system gradually increases from 25.9 °C in the first cycle to 30.6 °C in the sixth cycle (an increase of 18.1%). In terms of the PRW with only heat emission, natural recovery in the underground aquifer cannot restore it to its original state. In addition, an increase in the average pumping temperature affects the efficiency of the heat pump system. The annual increase in the pumping temperature must be examined only under heat emission conditions, and appropriate measures must be implemented in a timely manner to supply the cooling capacity to the underground aquifers.

Fig. 9 shows variations in the cumulative released heat of the PRW in the six cycles under continuous heat release condition. The cumulative released heat of the PRW decreases every year in the six cycles. In the six-year simulated system operation, the accumulated heat of the thermal source well gradually decreases from 9923.2 kJ in the first cycle to 9324.9 kJ in the sixth cycle (a reduction of 6.0%), and the average reduction in each cycle is 1%. Compared with a reduction of 23.0% in the cumulative extracted heat for the system operating mode in the Shenyang region in the six cycles, natural recovery be enhanced in the underground aquifer can. The thermal source well is more sensitive to heat extraction, which is more difficult to achieve than heat release. Therefore, heat introduced to supplement the aquifers must be examined.

3.3. Experimental characteristics in Shenyang

This section describes the results obtained during the heating and air conditioning periods in Shenyang in the six cycles in the SW and WS operation modes. First, the system operates in the SW operation mode during summer, then enters the natural recovery period, operates in the winter operation mode, and enters the recovery period. This process is repeated over six cycles. The WS operation mode is the first operation mode during winter, and the duration of each operation mode is listed in Table 3.

3.3.1. Summer winter operation mode – Shenyang

Fig. 10 shows variations in the pumping temperature of the PRW in Shenyang in the SW operation mode. As shown in the figure, the pumping temperature of the system gradually increases under summer heat emission operating conditions and gradually decreases under winter heat extraction operating conditions. The pumping temperature of the thermal source well varies between 14 °C and 21.5 °C under the six heat emission operating conditions, whereas a period of balance is achieved between heat extraction and load, that is, the pumping temperature is constant. However, the pumping temperature gradually decreases with increasing load.

Table 4 lists the initial and final pumping temperatures in the SW operation modes in the six stable running cycles. The pumping temperature increases or decreases during heat exchange. After heat emission, the pumping temperature of the thermal source well increases after gradually decreasing from 21.4 °C in the first cycle to 18.4 °C in the sixth cycle, indicating that heat emission

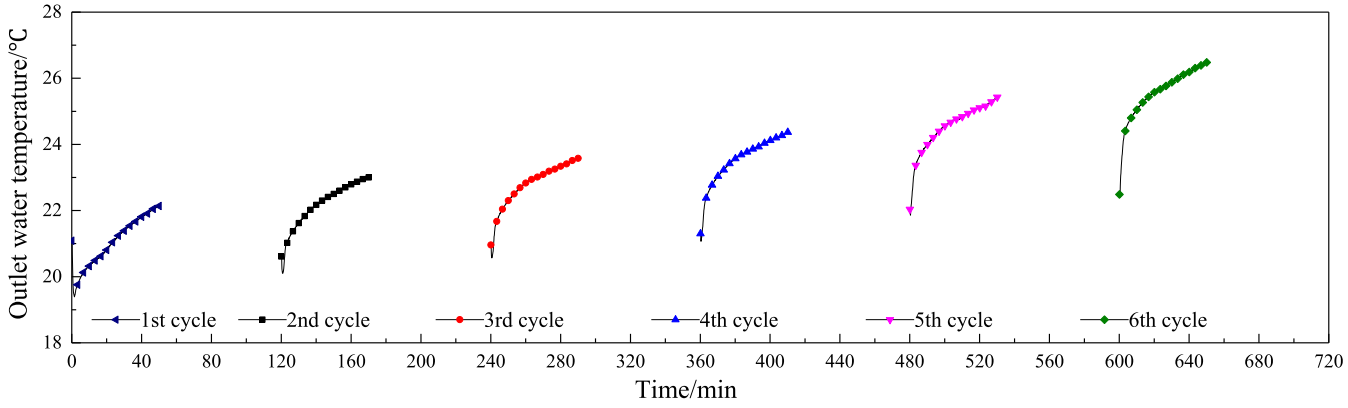

Fig. 7. Temperature of the outlet water under the continuous cooling (CC) condition.

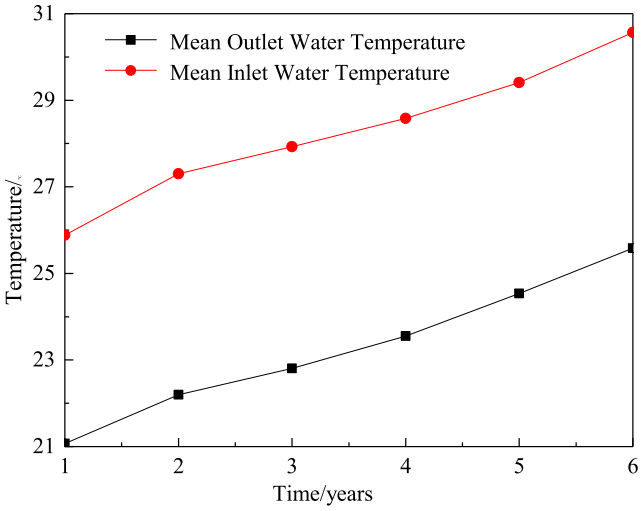

Fig. 8. Mean temperatures of the outlet and inlet water under the CC condition.

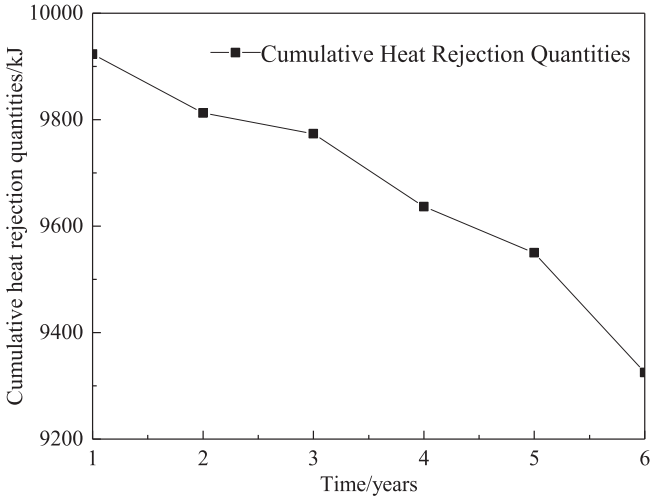

Fig. 9. Cumulative heat rejection quantities under the CC condition.

from the system does not restore the underground aquifer to its original state. After the natural recovery period during operation under heat extraction conditions, the initial and final pumping temperatures are similar under heat emission conditions. However, after operation under heat extraction conditions, the temperature of the pumping system gradually decreases from 16.7 °C in the first cycle to 15.1 °C in the sixth cycle. This indicates that the amount of heat extracted is higher than that emitted in a single cycle, which results in gradual yearly decrease in the pumping temperature. This can also be verified from the system heat exchange in each cycle listed in Table 4.

Fig. 11 shows variations in the average pumping temperature of the PRW in Shenyang in the SW operation mode. The average pumping temperature under heat emission conditions gradually decreases from 20.3 °C to 17.4 °C after six cycles of operation—a decrease of 2.9 °C. The average pumping temperature under heat

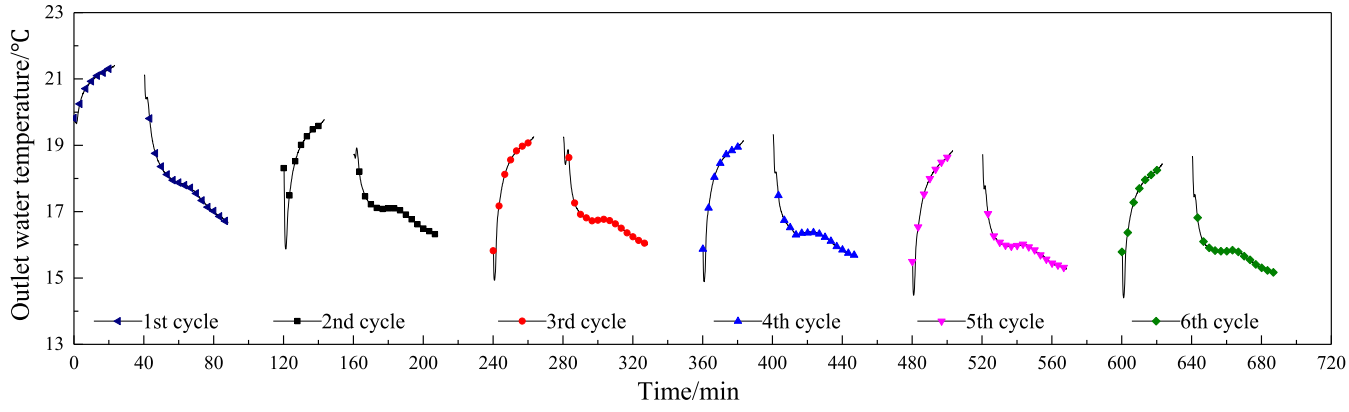

Fig. 10. Temperature of the outlet water in the first summer then winter (SW) operation mode in Shenyang.

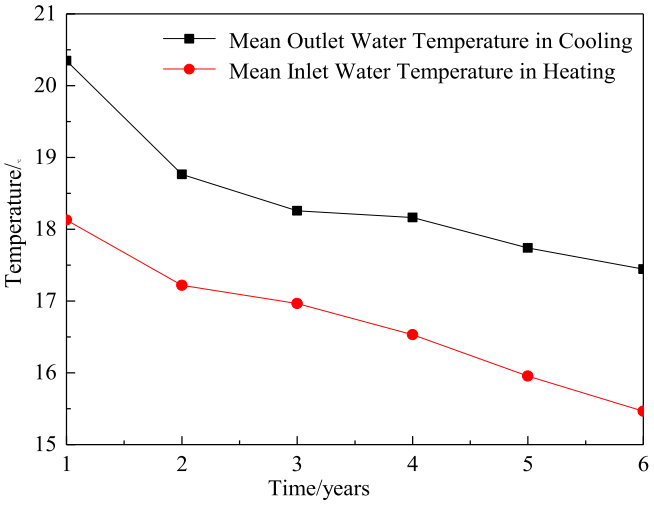

Fig. 11. Mean temperature of the outlet water in the SW operation mode in Shenyang.

extraction conditions gradually decreases from 18.1 °C to 15.4 °C after six cycles of operation—a decrease of 2.7 °C. It can be clearly observed that the average pumping temperature of the system decreases by approximately 2.8 °C after alternately running six cycles under heat emission or extraction conditions.

3.3.2. Winter summer operation mode – Shenyang

Fig. 12 shows variations in the pumping temperature of the PRW in Shenyang for the WS operation mode. The influences of the thermal source well under the WS and SW operation modes are similar: the pumping temperature of the system gradually decreases during winter operation and gradually increases during summer operation.

Fig. 13 shows variations in the pumping temperature of the PRW under the WS operation mode in Shenyang. The average pumping temperature under heat emission conditions decreases from 18.6 °C to 16.9 °C, representing a decrease of 1.7 °C, whereas the average pumping temperature under heat extraction conditions decreases from 17.7 °C to 15.5 °C, representing a decrease of 2.2 °C.

Table 4 also lists the initial and final pumping temperatures for the winter–summer operation mode in the six stable running cycles. The pumping temperature increases or decreases with heat exchange. The pumping temperature of the thermal source well gradually decreases during operation under heat extraction conditions from 16.7 °C in the first cycle to 14.8 °C in the sixth cycle. This indicates that the thermal source well continues extracting heat stored in the underground aquifer, resulting in a sharp decrease in the pumping temperature. After the natural recovery period, the initial pumping temperature of the system is 0.8 °C lower than the final pumping temperature when the system operates under the exothermic condition. However, the pumping temperature of the system increases by approximately 3.9 °C under heat emission conditions. The heat extracted by the system is higher than the heat emission in a single cycle, resulting in gradual decrease in the pumping temperature. This can be verified from the system heat exchange in each cycle as listed in Table 4.

3.3.3. Comparative analysis on operation modes – Shenyang

A comparison of the SW and WS operation modes of the PRW in Shenyang shows that the average pumping temperature in the six cycles is lower when the heating condition is applied first in winter compared with being applied first in summer. This is mainly because the underground aquifer stores a certain amount of heat energy and the heat extracted by the system is larger than the heat emission.

If the exothermic condition is applied first, the underground aquifer stores more heat under the CH condition. The sum of self-stored heat and exothermic heat reduces the heat lost during the recovery period. In this manner, the average pumping temperature of the thermal source well is higher when the heating condition is applied again. In contrast, if the system is operated under heat extraction conditions first, the thermal source well can extract only an equivalent amount of stored heat from the aquifer, resulting in a decrease in the average pumping temperature of the thermal source well. In an actual project, the system must be operated first under thermal emission conditions and then under heat extraction conditions in areas with dominant heating loads taking into consideration the running efficiency of the heat pump units to maintain the thermal source wells at a high pumping temperature.

3.4. Experimental characteristics in Beijing

This section describes the results obtained during the heating and air conditioning periods in Beijing in the six SW and WS cycles, with the durations of the other operation modes listed in Table 3.

3.4.1. Summer winter operation mode – Beijing

Fig. 14 shows variations in the pumping temperature of the PRW in Beijing over the six cycles for the SW operation mode. The pumping temperature of the thermal source well gradually increases under heat emission conditions and gradually decreases under heat extraction conditions. Under the six heat extraction cycles, the pumping temperature of the thermal source well varies between 17 °C and 20 °C, whereas the temperature range for the six heat emission cycles is wider than that of the heat extraction cycles.

Table 5 lists the initial and final pumping temperatures for the SW operation mode in the six stable cycles and the magnitude of the increase or decrease in the pumping temperature. The pumping temperature of the thermal source well increases to approximately 21.0 °C after operation under heat emission conditions, and the underground aquifer stores heat after system operation. After the natural recovery period, the initial and final pumping temperatures of the system are identical to those under heat emission conditions if the system operates under heat extraction conditions. However, under heat extraction conditions, the pumping temperature of the system decreases to approximately 17.3 °C. Under each operating condition, the system exhibits fluctuations in the pumping temperature, indicating that there is no considerable difference in the heat extraction and heat emission of the system in a single cycle. This can be verified from the variation in the heat exchange in each cycle as listed in Table 5.

Fig. 15 shows variations in the average pumping temperature of the PRW in Beijing for the SW operation mode. The average pumping temperature decreases from 20.8 °C to 19.4 °C under heat emission conditions after six alternating cycles, which represents a decrease of 1.4 °C, whereas the average pumping temperature under heat extraction conditions decreases from 18.5 °C to 18.2 °C after six alternating cycles, which represents a decrease of 0.3 °C. This indicates that variations in the average pumping temperature under heat extraction conditions are more stable compared with those under heat emission conditions and the average pumping temperature remains approximately 18.3 °C. This variation in the pumping temperature of the thermal source well is also evident from Fig. 14.

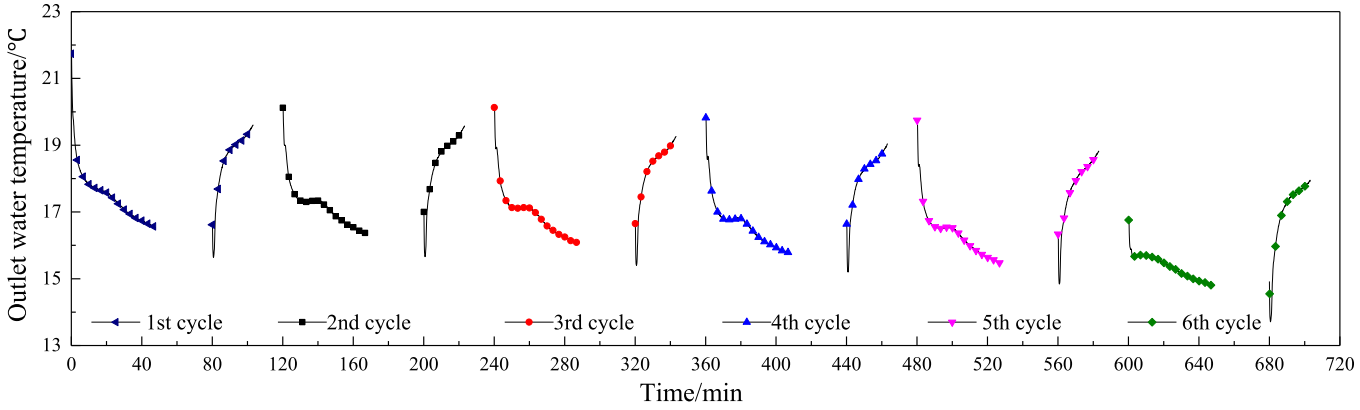

Fig. 12. Temperature of the outlet water in the first winter then summer (WS) operation mode in Shenyang.

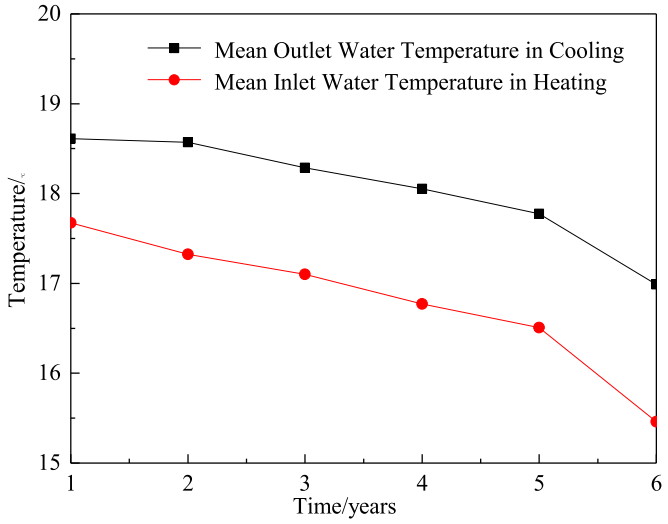

Fig. 13. Mean temperature of the outlet water in the WS operation mode in Shenyang.

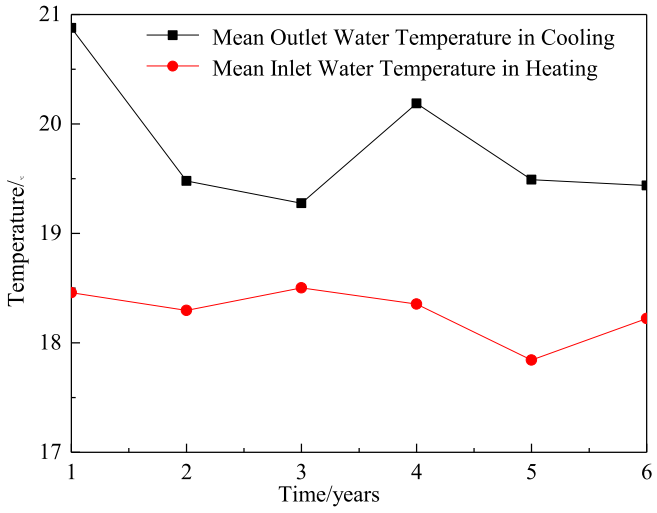

Fig. 15. Mean temperature of the outlet water in the SW operation mode in Beijing.

3.4.2. Winter summer operation mode – Beijing

Fig. 16 shows variations in the pumping temperature of the PRW in Beijing for the WS operation mode. The pumping temperature of the system gradually decreases during winter and gradually increases during summer. The pumping temperature of the thermal source well varies between 16.5 °C and 21.0 °C in the six cycles under heat emission conditions, whereas the pumping temperature varies between 15.3 °C and 24.0 °C in the six cycles under heat extraction conditions. The temperature range under heat extraction conditions is wider compared with that under heat emission conditions.

Fig. 17 shows variations in the average pumping temperature of the PRW in Beijing for the WS operation mode. The average

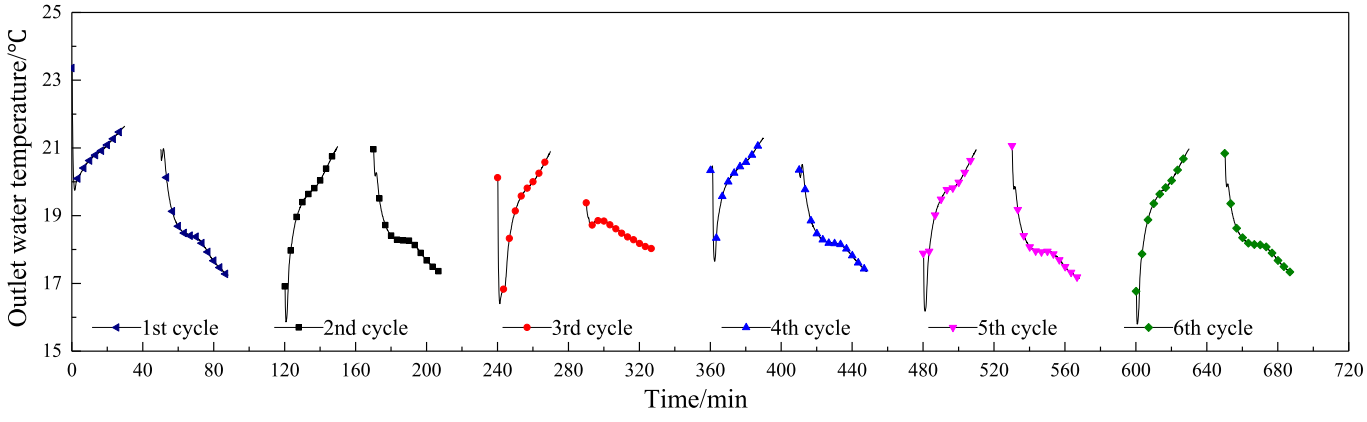

Fig. 14. Temperature of the outlet water in the SW operation mode in Beijing.

Table 5
Summary of the test results in Shenyang.

Period	Mode	Outlet water temperature-Begin (°C)	Outlet water temperature-End (°C)	Temperature difference (°C)	Cumulative heat absorption/rejection (kJ)
SW-1	S	19.7	21.4	−1.7	4838.3
	W	21.1	16.7	4.4	10,293.2
SW-2	S	15.9	19.8	−3.9	4976.1
	W	18.9	16.3	2.6	9765.5
SW-3	S	14.9	19.3	−4.4	5240.2
	W	19.2	16.0	3.2	8747.6
SW-4	S	14.9	19.1	−4.2	5340.9
	W	19.3	15.6	3.7	8859.4
SW-5	S	14.5	18.8	−4.3	4699.9
	W	18.7	15.3	3.4	8796.9
SW-6	S	14.4	18.4	−4.0	4913.9
	W	18.6	15.1	3.5	8014.7
WS-1	W	21.7	16.5	5.2	5701.1
	S	15.7	19.6	−3.9	4459.6
WS-2	W	20.1	16.4	3.7	5285.3
	S	15.7	19.6	−3.9	4480.4
WS-3	W	20.1	16.1	4.0	5200.4
	S	15.4	19.3	−3.9	4446.4
WS-4	W	19.8	15.7	4.1	5025.7
	S	15.2	19.0	−3.8	4473.8
WS-5	W	19.8	15.5	4.3	5295.3
	S	14.9	18.8	−3.9	5023.5
WS-6	W	16.7	14.8	1.9	5186.7
	S	14.0	18.0	−4.0	5026.6

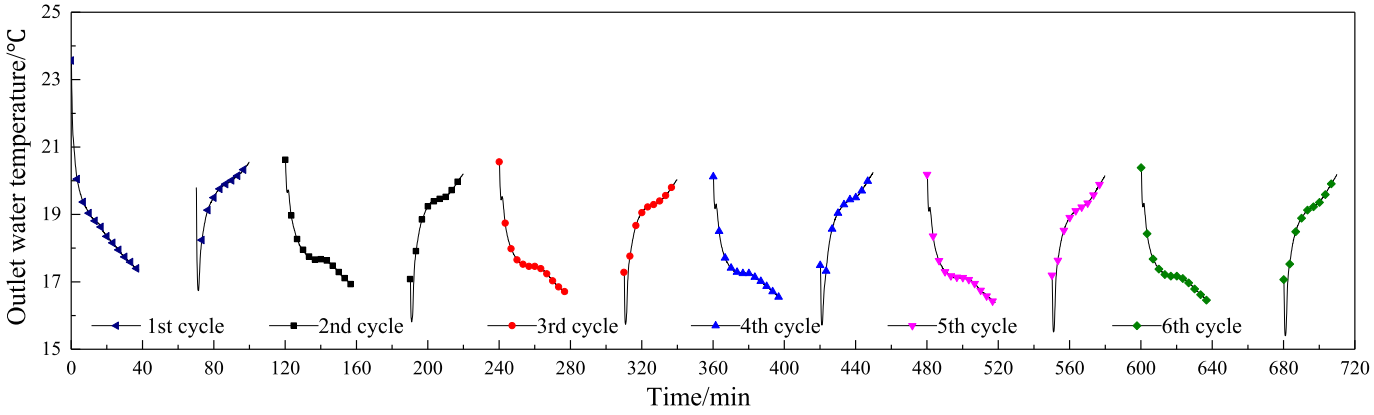

Fig. 16. Temperature of the outlet water in the WS operation mode in Beijing.

pumping temperature decreases from 19.6 °C to 18.9 °C in the six cycles under heat emission conditions, representing a decrease of only 0.7 °C, whereas the average pumping temperature decreases from 18.6 °C to 17.3 °C in the six cycles under heat extraction conditions, representing a decrease of 1.3 °C. It can be clearly observed that the average pumping temperature of the thermal source well varies slightly under heat emission conditions. This is consistent with the principle of operation of the thermal source well shown in Fig. 16.

Table 5 lists the initial and final stable pumping temperatures for the winter–summer operation mode in the six cycles and the magnitude of the increase or decrease in the pumping temperature and heat exchange. The pumping temperature of the thermal source well decreases to approximately 16.8 °C under heat extraction conditions, and the underground aquifer stores the cooling capacity of the system discharge.

After the natural recovery period, the initial pumping temperature of the system is approximately 1.0 °C lower than the final pumping temperature under heating condition when the system operates under exothermic conditions. However, the pumping temperature of the system increases to approximately 20.2 °C under heat emission conditions. The pumping temperature of the system fluctuates, which indicates that there is no considerable difference between heat emission and heat extraction in a single cycle; they are similar for the SW operation mode. This can also be verified from the variation in heat exchange in each cycle as presented in Table 5.

3.4.3. Comparative analysis of operation modes – Beijing

A comparison of the SW and WS operation modes of the PRW in Beijing shows that the pumping temperature in the winter heat extraction mode is relatively stable when the summer heat release mode is applied first, whereas the pumping temperature in the summer heat extraction mode is relatively stable when the winter heat extraction mode is applied first. In general, variations in the average pumping temperature are not high (less than 2 °C) regardless of heat extraction or emission conditions. If the CH and CC conditions are combined, operation under exothermic conditions results in heat discharge into the aquifer, which plays an important role in improving the operation in the next heating condition and storing part of the heat of the aquifer. Operation under the heating condition also improves the exothermic condition. This type of conversion of the working condition (corresponding to seasonal conversion of the actual engineering) can help utilize the cooling or heating capacity stored in the previous working condition (season) and play an important role in energy storage.

Table 6
Summary of the test results in Beijing.

Period	Mode	Outlet water temperature-Begin (°C)	Outlet water temperature-End (°C)	Temperature difference (°C)	Cumulative heat absorption/rejection (kJ)
SW-1	S	19.8	21.7	−1.9	5085.8
	W	20.9	17.2	3.7	6512.9
SW-2	S	15.8	21.0	−5.2	5788.3
	W	21.0	17.3	3.7	6426.0
SW-3	S	16.4	20.9	−4.5	4987.6
	W	19.4	18.0	1.4	4486.7
SW-4	S	17.7	21.3	−3.6	5465.7
	W	20.5	17.4	3.1	6871.7
SW-5	S	16.2	21.0	−4.8	6296.2
	W	21.1	17.2	3.9	6484.3
SW-6	S	15.8	20.9	−5.1	5938.2
	W	20.8	17.3	3.5	5813.5
WS-1	W	21.0	17.4	3.6	5904.7
	S	16.7	20.6	−3.9	6097.9
WS-2	W	20.6	16.9	3.7	6542.8
	S	15.8	20.2	−4.4	6334.3
WS-3	W	20.6	16.6	4.0	6455.6
	S	15.8	20.0	−4.2	6200.4
WS-4	W	20.1	16.5	3.6	6138.3
	S	15.7	20.2	−4.5	6399.5
WS-5	W	20.2	16.4	3.8	6235.4
	S	15.5	20.2	−4.7	6718.8
WS-6	W	20.4	16.4	4.0	6161.8
	S	15.4	20.2	−4.8	6817.7

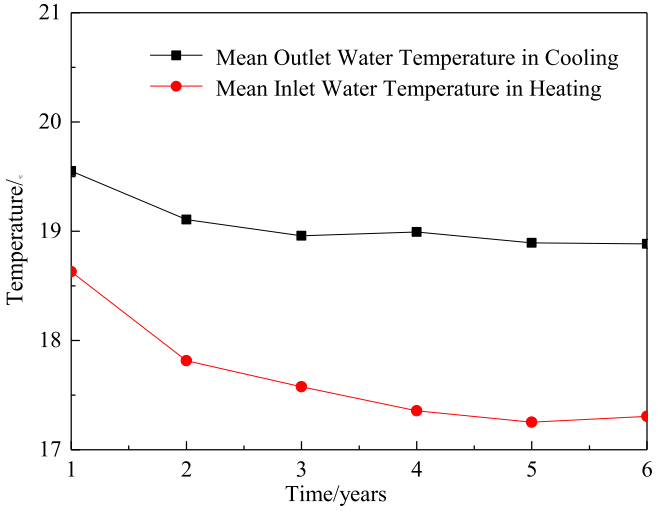

Fig. 17. Mean temperature of the outlet water in the WS operation mode in Beijing.

3.5. Experimental characteristics in Shanghai

This section describes the results obtained during the heating and air conditioning periods in Shanghai in the six cycles for the SW and WS operation modes. The durations of each operation mode are summarized in Table 3.

3.5.1. Summer winter operation mode – Shanghai

Fig. 18 shows variations in the pumping temperature of the PRW in Shanghai for the SW operation mode. The pumping temperature of the system gradually increases during summer and gradually decreases during winter. Fig. 19 shows variations in the average pumping temperature of the PRW in Shanghai for the SW operation mode. The average pumping temperature under heat emission conditions increases from 20.2 °C to 21.9 °C in the six cycles, representing an increase of 1.7 °C, whereas the average pumping temperature under heat extraction conditions increases from 18.8 °C to 21.9 °C in the six cycles, representing an increase of 2.5 °C.

Table 6 lists the initial and final pumping temperatures for the SW operation mode in the six stable cycles and the magnitude of the increase or decrease in the pumping temperature and heat exchange. The pumping temperature of the thermal source well gradually increases from 21.7 °C to 23.4 °C in the six cycles under heat emission conditions, indicating that heat emitted from the system increases the temperature of the aquifer. After the natural recovery period, the initial pumping temperature of the system is approximately 1.0 °C lower than the final pumping temperature under heat emission conditions. The pumping temperature increases from 18.0 °C to 20.8 °C in the six cycles under heat extraction conditions. This indicates that heat emission from the system is considerably higher than heat extraction for a single cycle, causing the pumping temperature to gradually increase. This can also be verified from the system heat exchange in each cycle as presented in Table 6.

3.5.2. Winter summer operation mode – Shanghai

Fig. 20 shows variations in the pumping temperature of the PRW in Shanghai for the WS operation mode. The pumping temperature of the system gradually decreases during winter but gradually increases during summer. Fig. 21 shows variations in the average pumping temperature of the PRW in the WS operation mode in Shanghai. The average pumping temperature under heat emission conditions increases from 20.2 °C to 21.3 °C in the six cycles, representing an increase of 1.1 °C, whereas the average pumping temperature under heat extraction conditions increases from 17.7 °C to 19.7 °C in the six cycles, representing an increase of 2.0 °C.

Table 6 lists the initial and final pumping temperatures for the WS operation mode in the six stable cycles and the magnitude of the increase or decrease in the pumping temperature and heat exchange. The pumping temperature of the thermal source well gradually increases from 17.3 °C to 19.2 °C in the six cycles under heat extraction conditions. After the natural recovery period, the initial pumping temperature of the system is approximately 1.0 °C lower than the final pumping temperature. The pumping temperature increases by approximately 4.5 °C under heat emission conditions. This indicates that heat emission from the system is higher than

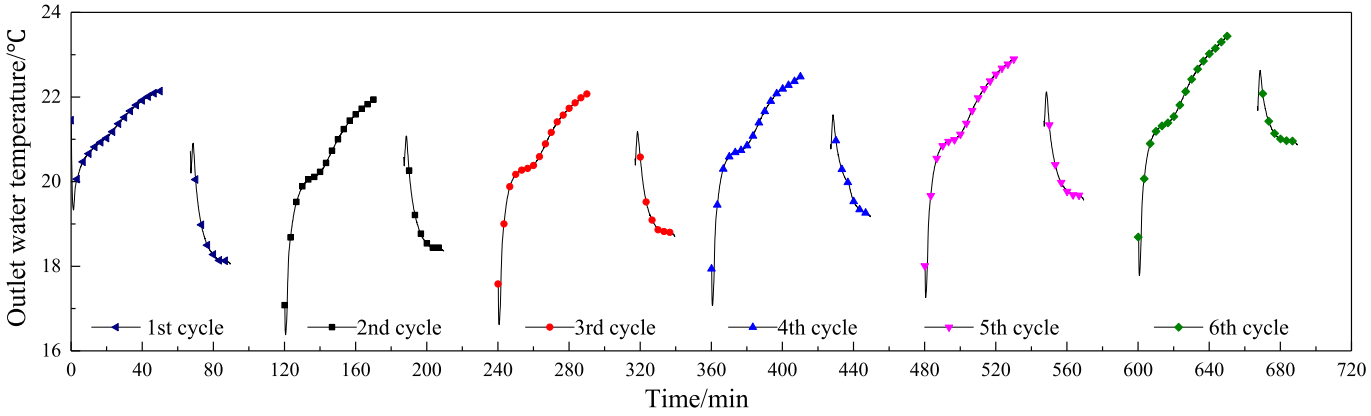

Fig. 18. Temperature of the outlet water in the SW operation mode in Shanghai.

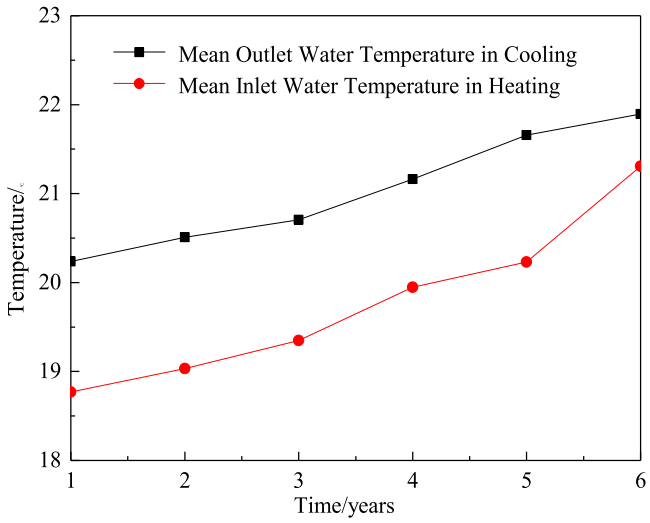

Fig. 19. Mean temperature of the outlet water in the SW operation mode in Shanghai.

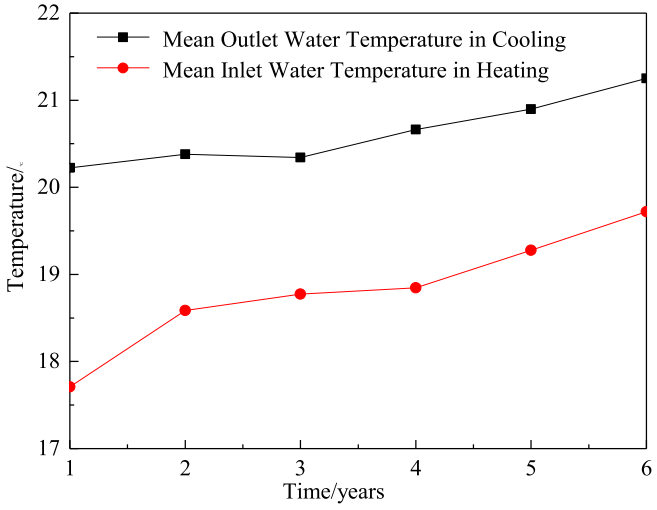

Fig. 21. Mean temperature of the outlet water in the WS operation mode in Shanghai.

heat extraction for a single cycle, causing a gradual increase in the pumping temperature. This can also be verified from the system heat exchange in each cycle as listed in Table 6.

3.5.3. Comparative analysis of operation modes – Shanghai

A comparison of the SW and WS operation modes of the thermal source well in Shanghai shows that the average pumping temperature in the six cycles is higher than the corresponding average pumping temperature in each working condition in winter. This is because the underground aquifer stores part of the heat. If the un-

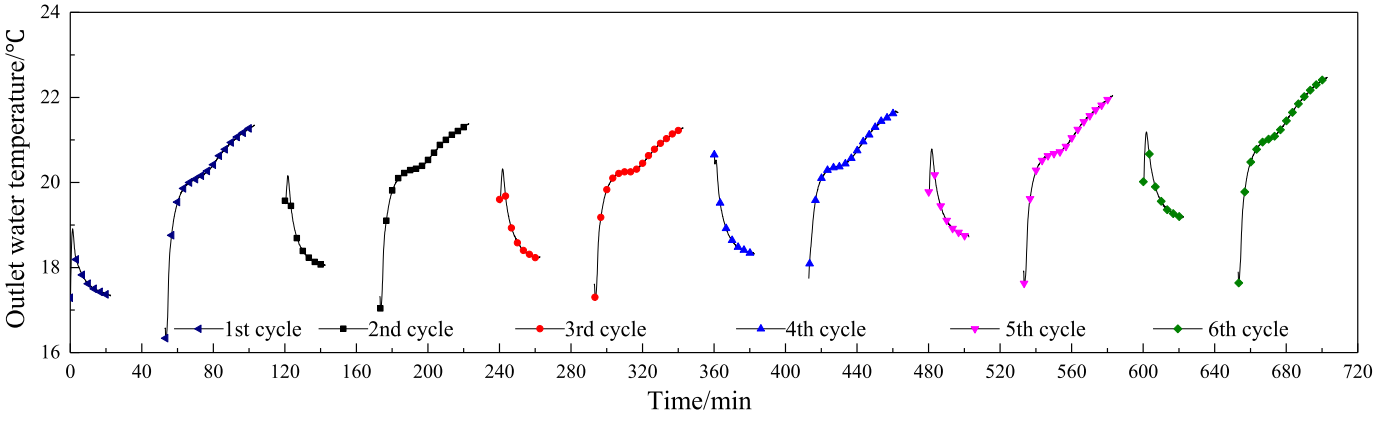

Fig. 20. Temperature of the outlet water in the WS operation mode in Shanghai.

Table 7
Summary of the test results in Shanghai.

Period	Mode	Outlet water temperature-Begin (°C)	Outlet water temperature-End (°C)	Temperature difference (°C)	Cumulative heat absorption/rejection (kJ)
SW-1	S	19.3	21.7	−2.4	10,253.1
	W	20.9	18.0	2.9	4988.2
SW-2	S	16.4	21.9	−5.5	9405.9
	W	21.0	18.4	2.6	5298.6
SW-3	S	16.6	22.0	−5.4	9911.9
	W	21.2	18.7	2.5	5050.3
SW-4	S	17.1	22.5	−5.4	9674.9
	W	21.6	19.2	2.4	4485.9
SW-5	S	17.3	22.9	−5.6	9394.3
	W	22.0	19.6	2.4	5325.3
SW-6	S	17.8	23.4	−5.6	9509.2
	W	22.6	20.8	1.8	3562.4
WS-1	W	18.9	17.3	1.6	3973.5
	S	16.3	21.3	−5.0	11,644.0
WS-2	W	20.1	18.1	2.0	4175.1
	S	17.0	21.4	−4.4	11,163.2
WS-3	W	20.3	18.3	2.0	4131.3
	S	17.2	21.3	−4.1	10,946.1
WS-4	W	20.6	18.3	2.3	4951.2
	S	17.4	21.6	−4.2	11,194.2
WS-5	W	20.8	18.7	2.1	4318.6
	S	17.6	22.0	−4.4	11,392.5
WS-6	W	21.2	19.2	2.0	4428.1
	S	17.7	22.5	−4.8	11,206.1

derground aquifer first operates under the heat release condition and then continues operating under the heat extraction condition, the heat stored in the aquifer is the sum of its heat, the heat released by the aquifer, and the heat lost during the recovery period, which is the reason for the higher pumping temperature of the thermal source well in the SW mode. However, in practical engineering projects, the heating condition must be applied first, followed by the heat release condition considering the actual operation efficiency of the heat pump units in cooling load-dominant areas in order to maintain the thermal source wells at a low pumping temperature (Table 7).

4. Conclusions

In this study, a sandbox test system of a single well underground heat exchange system was used to conduct experimental tests based on the duration of the heating and air conditioning periods in three representative cities (Beijing, Shenyang, and Shanghai) under four conditions, namely CH, CC, SW, and WS. The results obtained for different modes and long-term PRW operation complement in-depth research, guide the field application of PRWs, and allow the following conclusions to be drawn:

(1) During the operation of the PRW in heating load-dominant regions, the underground aquifer cannot restore itself to its original state in the natural recovery period under the experimental conditions, and assistive technology schemes must be utilized to supply heat to the underground aquifer to ensure long-term reliable operation of the system.
(2) During the operation of the PRW in cooling load-dominant moderate regions, the recovery of the underground aquifer is enhanced in the natural recovery period under the experimental conditions. Rapid heat loss occurs in the underground aquifer, the thermal source well easily removes heat under heat emission conditions, and it is difficult to extract heat under heat extraction conditions.
(3) In areas with similar heating and cooling loads, operating the PRW first under summer operating conditions and then under winter operating conditions improves heat extraction at later stages because of heat emission to the aquifer under heat emission conditions, which could release a portion of the heat to the aquifer. In heat load-dominant areas such as Shenyang, heat emission conditions must be implemented first, followed by heat extraction conditions, to maintain the thermal source wells at a high pumping temperature. In contrast, in cooling load-dominant areas such as Shanghai, heat extraction conditions must be implemented first, followed by thermal emission conditions, to maintain the thermal source wells at a low pumping temperature.

Declaration of Competing Interest

This manuscript has not been published or presented elsewhere in part or in entirety and is not under consideration by another journal. We have read and understood your journal's policies, and we believe that neither the manuscript nor the study violates any of these. There are no conflicts of interest to declare.

Acknowledgments

This work was supported by the National Natural Science Foundation of China (41002085, 41602278), China Postdoctoral Science Foundation (2016M601129), North China University of Technology Programs (XN018032, 18XN154-006, 18XN149), and NCUT One Belt-One Road National Talent Training Base (XN1805008) .

Supplementary materials

Supplementary material associated with this article can be found, in the online version, at doi:10.1016/j.enbuild.2019.109660.

References

[1] W. Song, L. Ni, Y. Yao, Experimental research on the characteristics of single-well groundwater heat pump systems, Energy Build. 191 (2019) 1–12.
[2] X. Bu, Y. Ran, D. Zhang, Experimental and simulation studies of geothermal single well for building heating, Renew. Energy 143 (2019) 1902–1909.
[3] C. Lee, J. You, H. Park, In-situ response test of various borehole depths and heat injection rates at standing column well geothermal heat exchanger systems, Energy Build. 172 (2018) 201–208.
[4] C. Lee, Thermal performance of a standing column well geothermal heat exchanger system using re-injection of bleeding water, Geothermics 82 (2019) 73–80.

[5] G. Wang, X. Song, Y. Shi, Baojiang Sun, Rui Zheng, Jiacheng Li, Zhijun Pei, Hengyu Song, Numerical investigation on heat extraction performance of an open loop geothermal system in a single well, Geothermics 80 (2019) 170–184.
[6] W. Song, L. Ni, Y. Yao, Experimental research on bleeding performance of single well ground-water heat pump, Procedia Eng. 205 (2017) 3162–3169.
[7] M.H. Jahangir, M. Ghazvini, F. Pourfayaz, et al., A numerical study into effects of intermittent pump operation on thermal storage in unsaturated porous media, Appl. Therm. Eng. 139 (2018) 110–121.
[8] Z. Jankovic, J. Sieres, F. Cerdeira, et al., Analysis of the impact of different operating conditions on the performance of a reversible heat pump with domestic hot water production, Int. J. Refrig. 86 (2018) 282–291.
[9] L. Kang, J. Yang, Q. An, et al., Complementary configuration and performance comparison of CCHP-ORC system with a ground source heat pump under three energy management modes, Energy Convers. Manag. 135 (2017) 244–255.
[10] W. Zhang, J. Jaromir, J.-K. Kim, Design and optimization of dual-mode heat pump systems using natural fluids, Appl. Therm. Eng. 43 (2012) 109–117.
[11] M.A. Sayegh, P. Jadwiszczak, B.P. Axcell, et al., Heat pump placement, connection and operational modes in European district heating, Energy Build. 166 (2018) 122–144.
[12] A. Agbossou, B. Souyri, B. Stutz, Modelling of helical coil heat exchangers for heat pump applications: analysis of operating modes and distance between heat exchangers, Appl. Therm. Eng. 129 (2018) 1068–1078.
[13] J. Cai, J. Ji, Y. Wang, et al., Operation characteristics of a novel dual source multi-functional heat pump system under various working modes, Appl. Energy 194 (2017) 236–246.
[14] H.W. Jung, H. Kang, H. Chung, et al., Performance optimization of a cascade multi-functional heat pump in various operation modes, Int. J. Refrig. 42 (2014) 57–68.
[15] A.M. Jalaluddin, Thermal performance investigation of several types of vertical ground heat exchangers with different operation mode, Appl. Therm. Eng. 33–34 (2012) 167–174.
[16] L. Dai, S. Li, L. DuanMu, et al., Experimental performance analysis of a solar assisted ground source heat pump system under different heating operation modes, Appl. Therm. Eng. 75 (2015) 325–333.
[17] B. Stojanovic, J. Akander, Build-up and long-term performance test of a full-scale solar-assisted heat pump system for residential heating in Nordic climatic conditions, Appl. Therm. Eng. 30 (2010) 188–195.
[18] F. Reda, A. Laitinen, Different strategies for long term performance of SAGSHP to match residential energy requirements in a cold climate, Energy Build. 86 (2015) 557–572.
[19] F. Reda, Long term performance of different SAGSHP solutions for residential energy supply in Finland, Appl. Energy 144 (2015) 31–50.
[20] X. Chen, L. Lu, H. Yang, Long term operation of a solar assisted ground coupled heat pump system for space heating and domestic hot water, Energy Build. 43 (2011) 1835–1844.
[21] M. Habibi, A. Hakkaki-Fard, Long-term energy and exergy analysis of heat pumps with different types of ground and air heat exchangers, Int. J. Refrig. 100 (2019) 414–433.
[22] H. Rehman, J. Hirvonen, K. Siren, A long-term performance analysis of three different configurations for community-sized solar heating systems in high latitudes, Renew. Energy 113 (2017) 479–493.
[23] B. Babak Dehghan, E. Kukrer, A new 1D analytical model for investigating the long term heat transfer rate of a borehole ground heat exchanger by Green's function method, Renew. Energy 108 (2017) 615–621.
[24] W. Li, X. Li, Y. Wang, J. Tu, An integrated predictive model of the long-term performance of ground source heat pump (GSHP) systems, Energy Build. 159 (2018) 309–318.
[25] W. Choi, R. Ooka, Y. Nam, Impact of long-term operation of ground-source heat pump on subsurface thermal state in urban areas, Sustain. Cities Soc. 38 (2018) 429–439.
[26] A. Capozza, A. Zarrella, M.D. Carli, Long-term analysis of two GSHP systems using validated numerical models and proposals to optimize the operating parameters, Energy Build. 93 (2015) 50–64.
[27] S. Li, K. Dong, J. Wang, X. Zhang, Long term coupled simulation for ground source heat pump and underground heat exchangers, Energy Build. 106 (2015) 13–22.
[28] H. Qian, Y. Wang, Modeling the interactions between the performance of ground source heat pumps and soil temperature variations, Energy Sustain. Dev. 23 (2014) 115–121.
[29] B. Li, Z. Han, X. Meng, H. Zhang, Study on the influence of the design method of the ground source heat pump system with considering groundwater seepage, Appl. Therm. Eng. 160 (2019) 114016.
[30] T. Kurevija, M. Macenic, S. Borovic, Impact of grout thermal conductivity on the long-term efficiency of the ground-source heat pump system, Sustain. Cities Soc. 31 (2017) 1–11.
[31] Q. Wu, K. Tu, H. Sun, C. Chen, Investigation on the sustainability and efficiency of single-well circulation (SWC) groundwater heat pump systems, Renew. Energy 130 (2019) 656–666.
[32] K. Tu, Q. Wu, H. Sun, A mathematical model and thermal performance analysis of single-well circulation (SWC) coupled ground source heat pump (GSHP) systems, Appl. Therm. Eng. 147 (2019) 473–481.
[33] N. Long, Operation performance research on heat source/sink well of groundwater heat pump with pumping & recharging in the same well, Harbin Inst. Technol. (2007).
[34] M.H. Sharqawy, E.M. Mokheimer, M.A. Habib, et al., Energy, exergy and uncertainty analyses of the thermal response test for a ground heat exchanger, Int. J. Energy Res. 33 (2009) 582–592.
[35] R.J. Moffat, Describing the uncertainties in experimental results, Exp. Therm. Fluid Sci. 1 (1) (1988) 3–17.